A biofuel cell based on two immiscible solvents and glucose oxidase and microperoxidase-11 monolayer-functionalized electrodes

Eugenii Katz, Boris Filanovsky and Itamar Willner*

Institute of Chemistry, The Hebrew University of Jerusalem, Jerusalem 91904, Israel

Received (in Strasbourg, France) 3rd November 1998, Accepted 15th February 1999

Apo-glucose oxidase was reconstituted onto a pyrroloquinoline quinone and flavin adenine dinucleotide phosphate (PQQ–FAD) monolayer associated with a rough Au electrode to yield a bioelectrocatalytically active glucose oxidase, GOx. An electrically contacted PQQ–FAD/GOx monolayer was applied for the biocatalytic oxidation of glucose in an aqueous electrolyte. Microperoxidase-11, MP-11, was assembled as a monolayer on a rough Au electrode and used for the biocatalytic reduction of cumene peroxide in a dichloromethane electrolyte solution. Both biocatalytic electrodes, Au/PQQ–FAD/GOx and Au/MP-11, were integrated into one system, creating a biofuel cell using glucose and cumene peroxide as the fuel substrate and the oxidizer, respectively, in a two-phase liquid system. The biofuel cell generates an open-circuit voltage, V_{oc}, of *ca.* 1 V and a short-circuit current density, i_{sc}, of *ca.* 830 μA cm^{-2}. The maximum electrical power, W_{max}, extracted from the cell is 520 μW at an external optimal load of 0.4 kΩ. The fill factor of the biofuel cell, $f = W_{max} \cdot I_{sc}^{-1} \cdot V_{oc}^{-1}$, is *ca.* 25%. The biofuel cell based on bioelectrocatalytic processes in two immiscible electrolytes shows a significant increase of the evaluated power in comparison with similar electrocatalytic systems in a single-phase aqueous electrolyte.

Biofuel cells use biocatalysts for the conversion of chemical energy to electrical energy.[1] As most organic substrates undergo combustion with the evolution of energy, the biocatalyzed oxidation of organic substances by oxygen at two electrode interfaces provides a means for the conversion of the chemical into electrical energy. Abundant organic raw materials such as methanol or glucose can be used as substrates for the oxidation processes at the anode, whereas molecular oxygen or H_2O_2 can act as the reduction substrates at the cathode. The extractable power (W) of a fuel cell is the product of the cell voltage (V_{cell}) and the cell current (I_{cell}). Although the ideal cell voltage is affected by the difference in the formal potentials of the oxidizer and fuel, irreversible losses in the voltage as a result of kinetic limitations of electron transfer at the electrode interfaces, ohmic resistances and concentration gradients, lead to decreased values of the cell voltage. Similarly, the cell current is controlled by the electrode sizes, the ion permeability and transport rate across the membrane separating the catholyte and anolyte compartments of the biofuel cell and, specifically, the rate of electron transfer at the respective electrode surfaces. These different parameters collectively influence the biofuel cell power, and for improved efficiencies the V_{cell} and I_{cell} values should be optimized.

Biofuel cells can use biocatalysts, enzymes or whole cell organisms for two different purposes.[2] (*i*) The biocatalysts can generate the fuel substrates for the cell by biocatalytic transformations or by metabolic processes. For example, the microorganism *Desulfovibrio desulfuricans* stimulates the metabolic reduction of sulfate to sulfide ions.[3] The latter product acts as the fuel substrate in the anodic compartment, where sulfide is being oxidized at the electrode interface to sulfate, and oxygen is being reduced in the cathodic compartment of the fuel cell. Other microorganisms were reported to yield hydrogen by their metabolic activities, and this product was used as the substrate for the conventional H_2/O_2 fuel cell.[4] Alternatively, a series of enzymes such as alcohol dehydrogenase, aldehyde dehydrogenase and formate dehydrogenase transform methanol to carbon dioxide with the concomitant reduction of the 1,4-nicotinamide adenine dinucleotide, NAD^+, cofactor to NADH.[5] The latter reduced cofactor was used as the fuel substrate of the anodic compartment of the fuel cell. (*ii*) The biocatalysts participate in the electron transfer chain between the fuel substrates and the electrode surfaces. That is, microorganisms, or redox enzymes, facilitate the electron transfer between the fuel substrate and the electrode interfaces, thereby enhancing the cell current. Most of the redox enzymes lack, however, direct electron transfer features with conductive supports, and a variety of electron mediators (electron relays) were used for the electrical contacting of the biocatalysts and the electrode.[6] For example, *N*-dimethyl-7-amino-1,2-benzophenoxazinium cation, MB^+, was used as an electron mediator in the glucose oxidase biocatalyzed oxidation of glucose in a glucose/O_2 fuel cell.[7] Glucose acts as the anodic fuel and its biocatalyzed oxidation to gluconic acid yields reduced glucose oxidase (GOx–$FADH_2$). The latter is oxidized by the electron mediator and the resulting electron carrier, MBH_2, supplies the electrons for the cathodic reduction of oxygen.

In recent years, our laboratory has been extensively involved in the functionalization of electrode surfaces with monolayers consisting of redox enzymes,[8] electrocatalysts[9] and bioelectrocatalysts[10] that stimulate electrocatalytic transformations at the electrode interfaces. Redox-active biomaterials were assembled on electrode supports and were used to activate biocatalytic electron transfer cascades, or to induce bioelectrocatalyzed transformations.[10] Reconstitution of apoflavoenzymes, such as apoglucose oxidase, onto an electron mediator–FAD monolayer associated with an electrode, led to aligned biocatalysts on electrode surfaces exhibiting effective and unprecedentedly efficient electrical contact.[11] Recently, we reported on the design of biofuel cells based on the biocatalyzed transformations at monolayer-modified electrodes.[12,13] The best results were achieved with a biofuel cell[13] based on glucose oxidation and hydrogen peroxide reduction in the anodic and cathodic compartments, respectively. Glucose oxidation was accomplished by the use of glucose oxidase reconstituted onto a relay–cofactor

* Fax +972 2 652 7715; e-mail: willnea@vms.huji.ac.il

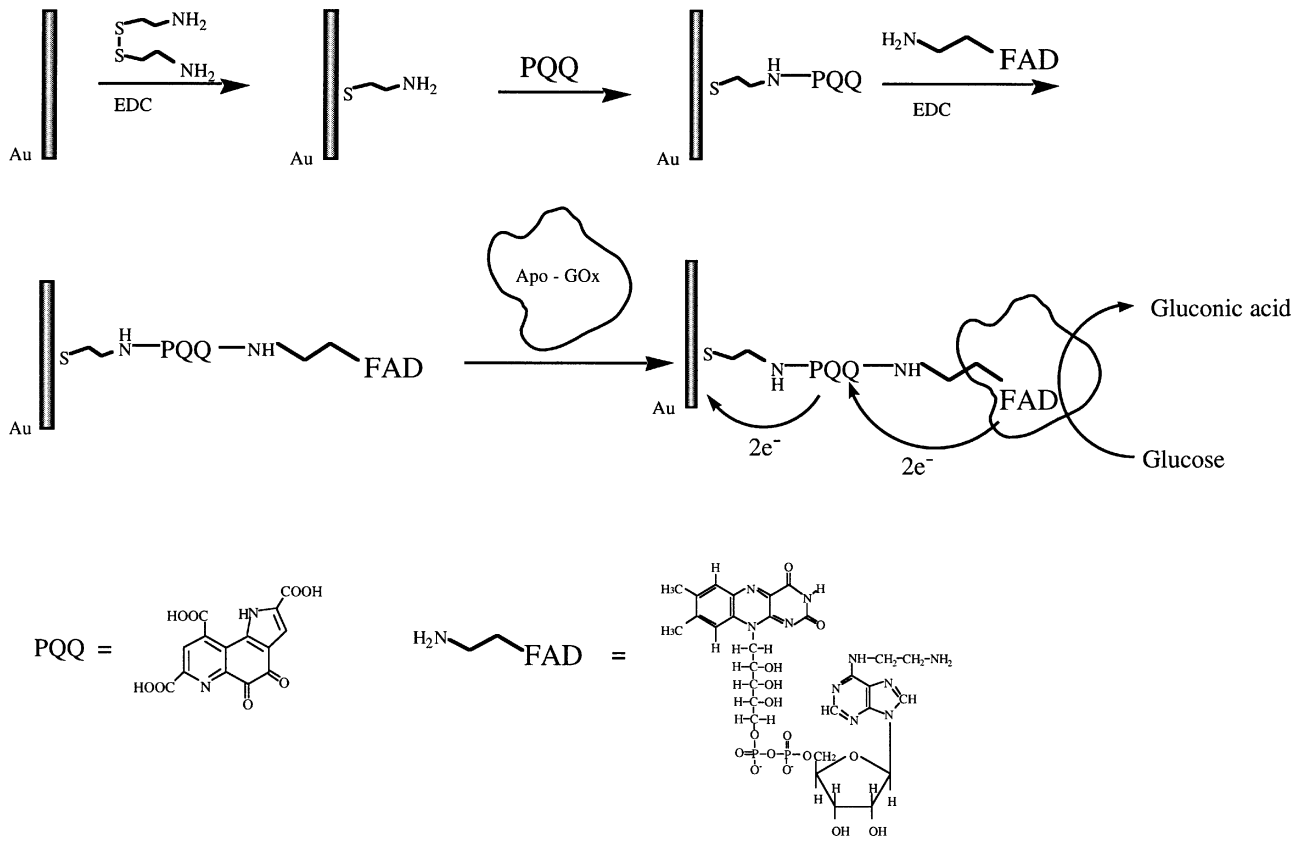

Scheme 1 Reconstitution of apo-glucose oxidase on the PQQ–FAD monolayer-functionalized electrode to yield an aligned glucose oxidase monolayer electrode.

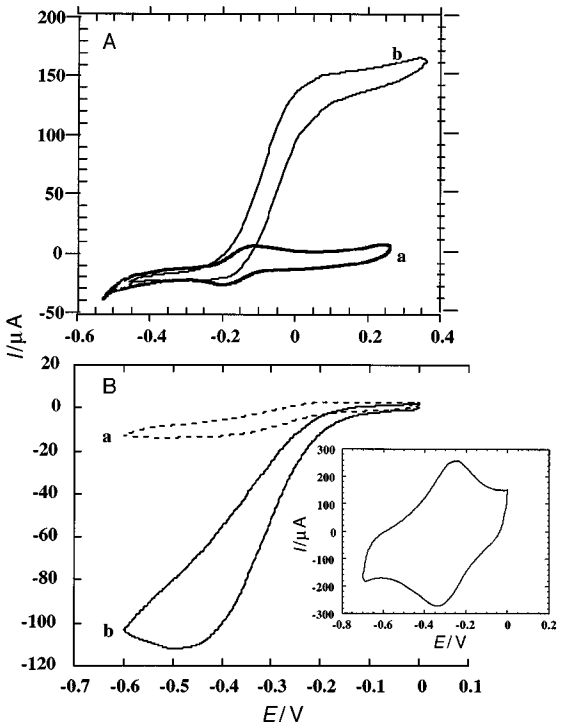

Fig. 1 (*A*) Cyclic voltammograms of reconstituted glucose oxidase on the PQQ–FAD monolayer associated with the gold electrode: (*a*) in the absence of glucose, (*b*) in the presence of added glucose, 5×10^{-3} M, and the PQQ–FAD reconstituted GOx electrode. Ar atmosphere, 0.01 M phosphate buffer, pH 7.0, and 0.05 M TBATFB. Potential scan rate, 5 mV s^{-1}. (*B*) Cyclic voltammograms of the MP-11-functionalized electrode: (*a*) *vs.* background electrolyte, (*b*) in the presence of cumene peroxide, 5×10^{-3} M. Potential scan rate, 5 mV s^{-1}. Inset: Cyclic voltammogram of the MP-11-monolayer-modified Au electrode in the absence of cumene peroxide. Potential scan rate, 50 mV s^{-1}; Ar atmosphere; electrolyte composed of a dichloromethane solution with 0.05 M TBATFB.

monolayer-functionalized electrode. Bioelectrocatalyzed reduction of hydrogen peroxide was stimulated in the catholyte compartment using a microperoxidase-11 (MP-11) monolayer-modified electrode. Both biocatalytic electrodes operated in aqueous electrolyte solutions separated by a porous membrane.

Further improvement of biofuel cells could be achieved either by the application of other biocatalytic systems or by the use of available bioelectrocatalytic assemblies that operate in new environments where the limiting factors of the cell performance are eliminated or reduced. Enzymes,[14] particularly peroxidases,[15] can function in non-aqueous solutions. Biocatalyzed reduction of hydroperoxides in the presence of peroxidase[15] can be applied as the cathodic process in a biofuel cell. A horseradish peroxidase-modified electrode was applied for the biocatalytic reduction of organic peroxides in non-aqueous solvents.[16] However, the biocatalytic activity of enzymes, particularly of horseradish peroxidase,[17] is usually lower (sometimes by an order of magnitude) in organic solvents, compared to aqueous solutions. Microperoxidase-11 monolayer-modified electrodes demonstrated high activity and stability for the electrocatalytic reduction of organic hydroperoxides in non-aqueous (acetonitrile and ethanol) solutions compared to the reduction in an aqueous solution.[9]

Charge transfer processes across the interface of two immiscible electrolyte solutions can mimic charge transfer reactions in living organisms. In nature, electron transfer processes frequently occur between redox centers that are located in media of different polarity. Many different systems with liquid–liquid intefaces have been studied using numerous experimental approaches.[18] Electrolysis at the interface between two immiscible electrolyte solutions has broad applications,[19] for example, in the basic understanding of biological membrane phenomena, the modelling of the operation of ion-selective electrodes based on liquid membranes,[20] phase transfer catalysis,[21] kinetic studies of solvent extraction processes,[22] *etc.*

However, to our knowledge, the liquid–liquid interface has never been applied as a liquid membrane separating cathodic and anodic processes in fuel cells.

Here we report on a novel biofuel cell configuration based on the biocatalyzed oxidation of glucose by cumene peroxide with the charge transfer occurring at the liquid–liquid interface of the immiscible solvents. The fuel cell consists of a glucose oxidase enzyme electrode generated by the reconstitution of the apo-protein on a pyrroloquinoline quinone–flavin adenine dinucleotide phosphate, PQQ–FAD, monolayer associated with an Au electrode. The resulting aligned enzyme on the electrode support is used as a bioelectrocatalytic interface for the oxidation of glucose in the aqueous anolyte compartment. A microperoxidase-11 monolayer assembled on an Au electrode is used as a catalytic electrode for the reduction of cumene peroxide in a dichloromethane solution acting as the catholyte compartment.

Results and discussion

The assembly of the aligned glucose oxidase, GOx, monolayer on a rough Au electrode (roughness factor *ca.* 20) is shown in Scheme 1. Prior to the reconstitution process, the functionalized monolayer shows[11] two reversible redox waves at $E^0 = -0.125$ V and $E^0 = -0.50$ V (at pH = 7.0), corresponding to the two-electron redox processes of PQQ and FAD, respectively. By integration of the charge associated with the PQQ and FAD redox units, the surface densities of these components were estimated to be *ca.* 1×10^{-11} mol cm^{-2}. Reconstitution of the enzyme on the PQQ–FAD monolayer yields a bioelectrocatalytically active monolayer interface for the bioelectrocatalyzed oxidation of glucose.[11] The surface density of the protein on the electrode surface was estimated[11] to be *ca.* 1.7×10^{-12} mol cm^{-2} (*vs.* real electrode area). Using the footprint dimension of GOx (58 nm^2),[23] the surface coverage of the electrode by the enzyme corresponds to a random densely packed enzyme monolayer assembly. Fig. 1(*A*) shows the cyclic voltammograms of the reconstituted-GOx-monolayer electrode in the absence and presence of added glucose (scan-rate 5 mV s^{-1}). With glucose, an electrocatalytic anodic current is observed, curve *b*, implying the effective bioelectrocatalyzed oxidation of glucose by the biocatalytic enzyme-monolayer electrode. The anodic current transduced by the reconstituted GOx-monolayer electrode is unprecedentedly high, and it is not affected by oxygen.[11] In a previous report[11] we estimated that the GOx biocatalyst reconstituted on the PQQ–FAD monolayer operates with a turnover rate of electron transfer (600 ± 100 s^{-1} at 25 °C) close to the value of the native enzyme with dioxygen as the electron acceptor.[24] This extremely efficient electrical contact of reconstituted apo-GOx with the electrode was attributed to the alignment of the biocatalyst on the conductive support and to the vectorial PQQ-mediated electron transfer between the FAD site and the electrode, Scheme 1. Oxidation of glucose by the biocatalyst yields the reduced $FADH_2$ redox site. The PQQ mediates oxidation of $FADH_2$ and is further regenerated by the electron transfer to the electrode. As the quinone is exposed to the electrode surface, its rapid oxidation by the conductive support enables the cyclic electrochemically induced oxidation of glucose. The following reaction scheme [eqn. (1)–(3)] accounts for the PQQ-mediated bioelectrocatalyzed glucose oxidation.

$$\text{Electrode–PQQ–FADH}_2\text{–GOx} \xrightarrow{k_{FAD-PQQ}} \text{Electrode–PQQH}_2\text{–FAD–GOx} \quad (1)$$

$$\text{Electrode–PQQH}_2\text{–FAD–GOx} \xrightarrow{k_{PQQ}} \text{Electrode—PQQ–FAD–GOx} + 2H^+ + 2e^- \text{ (to the electrode)} \quad (2)$$

$$\text{Electrode–PQQ–FAD–GOx} + \text{Glucose} \xrightarrow{k_{cat}} \text{Electrode–PQQ–FADH}_2\text{–GOx} + \text{Gluconic acid} \quad (3)$$

In this scheme $k_{FAD-PQQ}$, k_{PQQ} and k_{cat} represent the rate constants for the electron transfer from the reduced FAD to PQQ, from the reduced PQQ to the electrode, and the biocatalyzed reduction of FAD by glucose, respectively. It should be noted that previous reports[25] have addressed the electrical contacting of glucose oxidase with an electrode by the covalent attachment of electron-relay groups to the protein, or by the immobilization of the biocatalyst in a redox polymer. Nonetheless, these electrically contacted biocatalytic assembles are far less efficient than the aligned reconstituted glucose oxidase configuration.

Microperoxidase-11, MP-11, is an oligopeptide consisting of eleven amino acids and a covalently linked Fe^{III}–protoporphyrin IX heme site. The oligopeptide is obtained by the controlled hydrolytic digestion of cytochrome c and represents the structure of the active site microenvironment of cytochrome c.[26] The electrochemistry of microperoxidase-11 has been well studied.[27] We have previously reported on the assembly of an MP-11 monolayer on an Au electrode,[28,29] and on the bioelectrocatalytic features of this monolayer in the reduction of H_2O_2 [28] and organic peroxides.[9] Scheme 2 shows the method to assemble the MP-11-monolayer electrode. It consists of the covalent coupling of the oligopeptide to a base cystamine monolayer in the presence of EDC. Previous mechanistic studies[29] indicate that MP-11 is linked to the electrode by two different configurations. One configuration involves the covalent linkage of a glutamate carboxylic acid residue to the base cystamine monolayer, whereas the

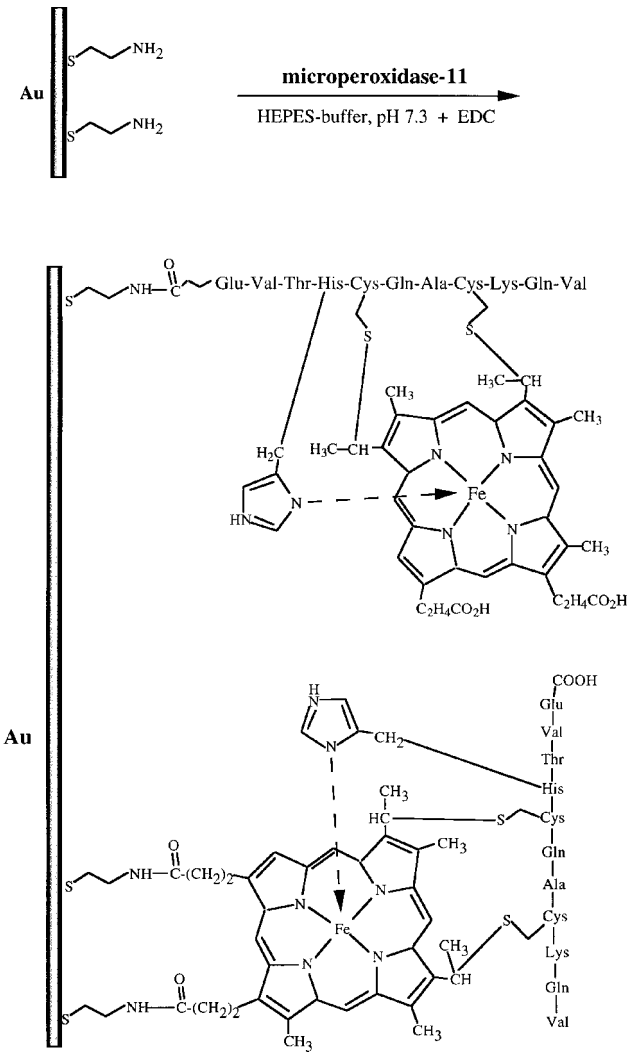

Scheme 2 Assembly of the MP-11-monolayer-modified electrode.

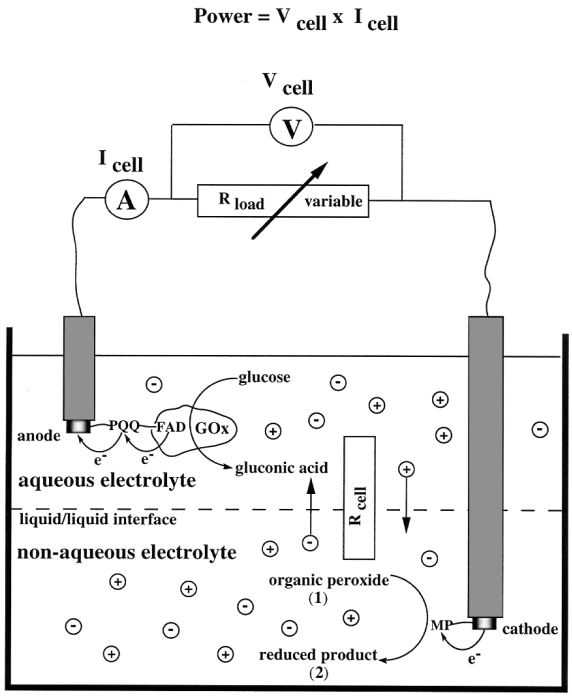

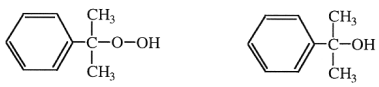

(1) (2)

Scheme 3 Schematic configuration of a biofuel cell operating in a two-phase liquid system employing glucose and cumene peroxide, **1**, as the fuel and oxidizer, respectively, and PQQ–FAD/GOx- and MP-11-functionalized electrodes as the biocatalytic anode and cathode, respectively, separated by a liquid–liquid interface.

second configuration includes the covalent attachment of carboxylic acid residues linked to the porphyrin site. Fig. 1(*B*) (inset) shows the cyclic voltammogram of the resulting MP-11 monolayer in a dichloromethane electrolyte. A quasi-reversible redox wave of the heme center of MP-11 is observed at $E^{\circ} = -0.30$ V (*vs.* aqueous SCE). Coulometric assaying of the redox wave indicates a surface coverage of *ca.*

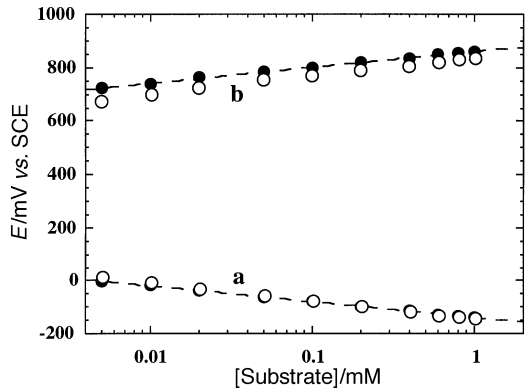

Fig. 2 (*a*) Potential of the PQQ–FAD/GOx-modified electrode as a function of glucose concentration in 0.01 M phosphate buffer, pH 7.0, and 0.05 M TBATFB. (*b*) Potential of the MP-11-functionalized electrode as a function of cumene peroxide concentration in a dichloromethane solution, 0.05 M TBATFB. Potentials were measured *vs.* aqueous SCE: (●) potentials measured in solutions saturated with air, (○) potentials measured in solutions after bubbling of argon. Note that for (*a*) the potentials measured with air and Ar almost coincide.

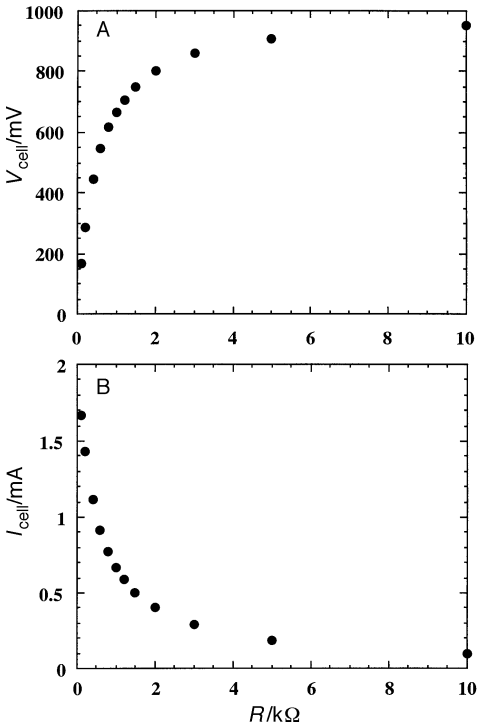

Fig. 3 (*A*) Biofuel cell voltage at different external loads. (*B*) Current developed by the cell at different external loads. Data recorded using the PQQ–FAD/GOx- and MP-11-functionalized electrodes and cumene peroxide, 1×10^{-3} M, as the substrate solution in the cathodic compartment, and glucose, 1×10^{-3} M, as the substrate solution of the anodic compartment. The background electrolyte in the anodic compartment was aqueous 0.01 M phosphate buffer, pH 7.0, and 0.05 M TBATFB. The background electrolyte in the cathodic compartment was a dichloromethane solution with 0.05 M TBATFB.

3×10^{-10} mol cm^{-2} (*vs.* real electrode area). Fig. 1(*B*) shows the cyclic voltammograms of the MP-11-functionalized electrode in the absence of an organic peroxide (curve *a*), and in the presence of added cumene peroxide, **1** (curve *b*). The observed electrocatalytic cathodic current indicates the effective bioelectrocatalyzed reduction of cumene peroxide by the functionalized electrode. The sequence of electron transfers leading to the reduction of the peroxide is summarized in eqn. (4) and (5)

$$\text{Electrode–MP-11(Fe}^{3+}\text{)} \xrightarrow{k_{\text{MP-11}}} \text{Electrode–MP-11(Fe}^{2+}\text{)} \quad (4)$$

$$\text{Electrode–MP-11(Fe}^{2+}\text{)} + \text{Cumene peroxide, } \mathbf{1} \xrightarrow{k_{\text{cat}}} \text{Electrode–MP-11(Fe}^{3+}\text{)} + \text{Cumene alcohol, } \mathbf{2} \quad (5)$$

In these reactions $k_{\text{MP-11}}$ and k_{cat} represent the rate constants of the electrochemical reduction of MP-11 and further catalytic reduction of the organic peroxide by the reduced state of MP-11, respectively.

The electrocatalyzed reduction of cumene peroxide by the MP-11-monolayer electrode and the effective bioelectrocatalyzed oxidation of glucose by the reconstituted-GOx-monolayer electrode enables us to design a biofuel cell using cumene peroxide and glucose as the cathodic and anodic substrates, respectively, and to operate in two immiscible electrolyte solutions, as shown in Scheme 3. The MP-11-monolayer electrode acts as the cathode, whereas the GOx-monolayer electrode is the anode of the biofuel element. For the optimization of the biofuel cell element, the potentials of the monolayer-modified electrodes as a function of the concentration of the cathodic and anodic substrates were determined *versus* the aqueous SCE reference electrode. Fig. 2 shows the potential of the GOx-monolayer electrode at different concen-

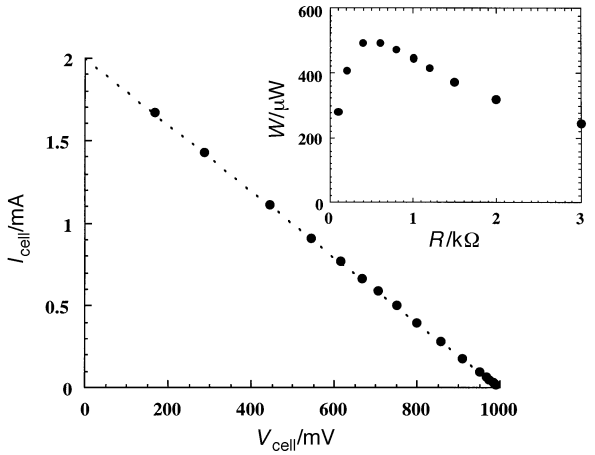

Fig. 4 Current–voltage behavior of the biofuel cell. Inset: Electrical power extracted from the biofuel cell at different external loads.

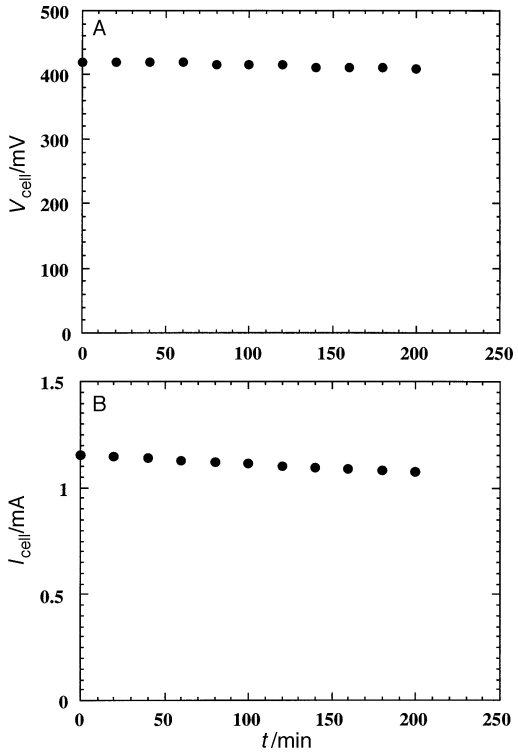

Fig. 5 Stability of the biofuel cell output: (*A*) voltage and (*B*) current, as a function of time upon operation of the cell at the optimal load of 0.4 kΩ.

trations of glucose in the aqueous electrolyte solution (curve *a*) and the potential of the MP-11-monolayer electrode at different concentrations of cumene peroxide in the dichloromethane electrolyte solution (curve *b*). The potentials of the GOx-monolayer electrode and of the MP-11-monolayer electrode become more negative and more positive, respectively, as the concentrations of the glucose and cumene peroxide are respectively elevated. The potentials of the electrodes reveal Nernstian-type behavior, showing a logarithmic increase and reaching saturation at a high concentration of the substrates. For our specific system, the saturation potentials of the anode and cathode are reached at *ca.* 1×10^{-3} M of glucose and 1×10^{-3} M of cumene peroxide, respectively. From the saturated potential values of the GOx- and MP-11-monolayer electrodes, the theoretical limit of the open-circuit voltage of the cell is estimated to be *ca.* 1 V. It should be noted that the potentials extrapolated to zero concentrations of the substrates show a large difference, *ca.* 700 mV, which results from the potential jump at the liquid–liquid interface. The potentials of both biocatalytic electrodes were measured in solutions saturated with air and after bubbling of argon. In the case of the GOx-monolayer electrode (anode), the presence of dioxygen in solution does not affect the potential developed by the electrode since the vectorial electron transfer from GOx to the electrode *via* the PQQ mediator competes successfully with the electron transfer from GOx to dioxygen.[11] The potential developed by the microperoxidase-11-monolayer-modified electrode (cathode) is slightly more positive in the presence of dioxygen since both oxidizers, cumene peroxide and O_2, are reduced by the electrode. However, the difference between the potentials developed by the cathode in the presence and absence of O_2 is insignificant, especially when the cumene peroxide concentration is higher than 0.1 M. Since the effect of O_2 on the function of the biofuel cell is not significant, we studied the cell operation in the presence of O_2.

The biofuel cell performance was examined at the concentration corresponding to 1×10^{-3} M of each of the two substrates: fuel and oxidizer. Fig. 3(*A*) shows the cell voltage at variable external loads. The cell voltage first increases and then levels off, at an external load of *ca.* 5 kΩ, to a constant value of *ca.* 1 V. It should be emphasized that the high voltage developed by the cell results from the potential difference existing at the liquid–liquid interface. Fig. 3(*B*) shows the resulting current in the cell at variable external loads. Upon increase of the external load, the current drops and almost reaches zero at an external load of 10 kΩ. Fig. 4 shows the current–voltage behavior of the biofuel cell at different external loads. The ideal voltage–current relationship for an electrochemical generator of electricity is rectangular.[30] The linear

Table 1 Characteristic parameters of biofuel cells based on Au electrodes modified with biocatalyst monolayers

Cathodic biocatalyst	Oxidizer	Anodic biocatalyst	Fuel	Open-circuit voltage, V_{oc}/mV	Short-circuit current density, i_{sc}/μA cm^{-2}	Electrical power at optimal resistance/μW	Optimal loading resitance/kΩ	Electrolyte system	Catholyte/anolyte separation	Reference
Microperoxidase-11	H_2O_2	PQQ	NADH	320	30	8	3	0.1 M Tris-HCl buffer, pH 8.0, +0.02 M $CaCl_2$	Glass frit	12
Microperoxidase-11	H_2O_2	PQQ–FAD reconstituted GOx	Glucose	310	114	32	2	0.1 phosphate buffer, pH 7.0	Glass frit	13
Microperoxidase-11	Cumene peroxide	PQQ–FAD reconstituted GOx	Glucose	990	830	520	0.4	Dichloromethane +0.05 TBATFB/aqueous 0.01 M posphate buffer, pH 7.0	Liquid–liquid interface	Present work

dependence observed for the biofuel cell has a significant deviation from ideal behavior and yields a fill factor for the biofuel cell, $f = W_{max} \cdot I_{sc}^{-1} \cdot V_{oc}^{-1}$, equal to *ca.* 25%. The theory of the various types of overvoltages that produce non-rectangular *V–I* relationships has been addressed in detail by Vetter[31] and Delahay.[32] In the present case, the observed deviation results from mass transport losses,[31,32] reducing the cell voltage below its reversible thermodynamic value. The power extracted from the biofuel element ($W = V_{cell} \cdot I_{cell}$) is shown in Fig. 4 (inset) for different external loads. The maximum power corresponds to 520 μW at an external load of 0.4 kΩ.

The stability of the biofuel cell was examined as a function of time at an optimal loading resistance of 0.4 kΩ (Fig. 5). The voltage and current generated by the cell decrease by *ca.* 4% and 8%, respectively, after *ca.* 3 h of cell operation. This decrease in the cell power is attributed mainly to the depletion of the fuel and the oxidizer substrates. Thus, the biofuel cell demonstrated quite good stability. Comparison of characteristic parameters of the biofuel cell with recently published systems (Table 1) reveals the significant improvement achieved in the present system.

Conclusions

The present paper describes the use of monolayer-functionalized electrodes as catalytic interfaces for the organization of fuel cell elements. Specifically, it addresses the use of a glucose oxidase layer reconstituted onto a pyrroloquinoline quinone and flavin adenine dinucleotide phosphate, PQQ–FAD, monolayer, associated with a rough Au electrode as a bioelectrocatalytic interface for the oxidation of glucose. The system consists of the glucose-oxidase-monolayer electrode acting as anode, and a microperoxidase-11-monolayer electrode acting as cathode. The glucose-oxidase-monolayer electrode drives the bioelectrocatalyzed oxidation of the glucose fuel substrate, whereas the microperoxidase-11 acts as the cathode for the biocatalyzed reduction of cumene peroxide. The cell operates in a two-phase system consisting of two immiscible electrolytes and the liquid–liquid interface. Any hydroperoxide can be used in the system as long as it is soluble in the organic oil phase, but insoluble in water. The phase separation of the fuel and oxidizer is the basic concept for the enhanced efficiency of the cell. The cell revealed an open-circuit voltage of *ca.* 1 V and a short-circuit current density of *ca.* 830 μA cm^{-2}. The maximum power output of the cell is 520 μW at an optimal loading resistance of 0.4 kΩ.

Experimental

Apo-glucose oxidase, apo-GOx, was prepared by a modification of the reported method.[33] The glucose oxidase, GOx (from *Aspergillus niger*, E.C. 1.11.3.4), was dissolved in 0.025 M sodium phosphate buffer, pH = 6.0, 3 mL, that included 30% glycerol (v/v). The solution was cooled to 0 °C and acidified to pH = 1.7 with a 0.025 M sodium phosphate–H_2SO_4, pH = 1.1, that included 30% glycerol. The resulting solution was loaded on a Sephadex G-25 column (1.6 × 22 cm). The protein was eluted with 0.1 M sodium phosphate solution, pH = 1.7, that included 30% glycerol. The eluted fractions were spectrophotometrically analyzed (λ = 280 nm) and the samples containing the protein were combined. Dextran-coated charcoal was added to the protein solution. The pH of the mixture was adjusted to pH = 7.0 with 1 M NaOH and the solution was stirred for 1 h at 4 °C. The resulting solution was centrifuged (3400 rpm for 5 min) and filtered through a 0.45 μm filter. The resulting solution was dialyzed against a 0.1 M sodium phosphate buffer solution, pH = 7.0.

An amino-functionalized FAD derivative, N^6-(2-aminoethyl)-FAD, was synthesized according to the recently published procedure.[34] Pyrroloquinoline quinone (PQQ), microperoxidase-11, (MP-11), cystamine, 1-ethyl-3-(3-dimethylaminopropyl)carbodiimide (EDC) and all other reagents and solvents were purchased from Aldrich. Ultrapure water from a Nanopure (Barnstead) source was used throughout this work.

Gold electrodes (0.4 cm diameter disks, embedded in Teflon holders) were used for electrochemical measurements. Prior to the modification and measurements, they were cleaned according to a published technique[35] and roughened by treatment with mercury, followed by dissolution of the amalgam layer in nitric acid.[36] Cleanness of the electrodes and roughness coefficients of their surfaces were determined by cyclic voltammetry in 0.1 M H_2SO_4.[37] Typical roughness coefficients of the electrode surfaces after roughening were *ca.* 20. The electrode modification with a base cystamine monolayer, and further covalent coupling of the PQQ, was performed according to the published procedure.[36] The covalent coupling of the N^6-(2-aminoethyl)-FAD to the PQQ-monolayer-modified electrode was performed by soaking the electrodes in HEPES [4-(2-hydroxyethyl)piperazine-1-ethanesulfonic acid, sodium salt] buffer solution (0.1 M, pH = 7.2) that contained 5×10^{-4} M N^6-(2-aminoethyl)-FAD and 1×10^{-3} M EDC for 2 h at room temperature. Then the electrodes were thoroughly rinsed with water, examined with cyclic voltammetry, and used for reconstitution of the apo-GOx. The reconstituted GOx-monolayer electrodes[11] were prepared by treatment of the FAD–PQQ-monolayer-modified electrodes with the apo-GOx, 4 mg mL^{-1}, in 0.1 M phosphate buffer, pH = 7.0, for 4 h at 25 °C and 12 h at 4 °C. The electrodes were then rinsed by shaking in 0.1 M phosphate buffer, pH = 7.0, at 4 °C for 1 h to eliminate any non-specific adsorbates.

Amino groups of the adsorbed cystamine monolayer were used for covalent coupling with carboxylic functions of the microperoxidase-11 in the presence of EDC in 0.05 M HEPES buffer, pH 7.3, for 2 h according to published procedures.[28,29]

The PQQ–FAD/reconstituted-GOx- and MP-11-monolayer-modified electrodes were characterized by applying cyclic voltammetry using a potentiostat (EG&G VersaStat) connected to a personal computer (EG&G research electrochemistry software model 270/250). Cyclic voltammetry was performed under argon at room temperature in a three-compartment electrochemical cell consisting of the glucose-oxidase- or MP-11-modified electrode as the working electrode, a glass carbon auxiliary electrode isolated by a glass frit, and a saturated calomel electrode (SCE) connected to the working volume with a Luggin capillary. Cyclic voltammetry study of the GOx-modified Au electrode was performed in an aqueous electrolyte solution composed of 0.01 M phosphate buffer, pH 7.0, and 0.05 M tetrabutylammonium tetrafluoroborate (TBATFB). A dichloromethane solution of 0.05 M TBATFB was used as a background electrolyte for the cyclic voltammetry study of the MP-11-modified Au electrode. Cyclic voltammograms and potentiometric measurements for each modified electrode, in the presence of the corresponding substrate (glucose for the PQQ–FAD/reconstituted GOx electrode and cumene peroxide, **1**, for the MP-11-modified electrode) are reported *vs.* an aqueous SCE.

The PQQ–FAD/reconstituted-GOx-modified electrode was immersed into the aqueous 0.01 M phosphate buffer, pH 7.0 (upper layer) and the MP-11-modified Au electrode was immersed into the dichloromethane, 0.05 M TBATFB electrolyte (lower layer). The substrates (glucose and cumene peroxide) were added to the corresponding compartments of the cell. Air dissolved in the electrolyte solutions was not removed by any means. The voltage and the current generated by the cell were measured between the two modified electrodes by applying an external variable load resistance and by using a Keithley Autoranging Microvolt DMM (Model 197) for the respective voltage and current measurements.

Acknowledgements

This work was supported by the Belfer Foundation. We thank Mrs. V. Heleg-Shabtai for the preparation of apo-GOx.

References

1 (*a*) G. Prentice, *CHEMTECH*, 1984, **14**, 684. (*b*) G. Tayhas, R. Palmore and G. M. Whitesides, in *Enzymatic Conversion of Biomass for Fuels Production*, ACS Symposium Series No. 566, American Chemical Society, Washington, DC, ch. 14, 1994, pp. 271–290. (*c*) K. Kordesch, *Ber. Bunsenges. Phys. Chem.*, 1990, **94**, 902. (*d*) C. Van Dijk, C. Laane and C. Veeger, *Recl. Trav. Chim. Pays Bas*, 1985, **104**, 245. (*e*) S. Suzuki, I. Karube, H. Matsuoka, S. Ueyama, H. Kawakubo, S. Isoda and T. Murahashi, *Ann. N. Y. Acad. Sci.*, 1983, **413**, 133.

2 (*a*) E. V. Plotkin, I. J. Higgins and H. A. O. Hill, *Biotechnol. Lett.*, 1981, **3**, 187. (*b*) W. J. Aston and A. P. F. Turner, *Biotechnol. Genet. Eng. Rev.*, 1984, **1**, 89. (*c*) C. Laane, W. Pronk, M. Franssen and C. Veeger, *Enzyme Microbiol. Technol.*, 1984, **6**, 165. (*d*) H. P. Bennetto, G. M. DeLaney, J. R. Mason, S. D. Roller, J. L. Stirling and C. F. Thurston, *Biotechnol. Lett.*, 1985, **7**, 699. (*e*) C. A. Vega and I. Fernandez, *Bioelectrochem. Bioenerg.*, 1987, **17**, 217. (*f*) S. Tanisho, N. Kamiya and N. Wakao, *Bioelectrochem. Bioenerg.*, 1989, **21**, 25. (*g*) D. Sell, P. Kraemer and G. Kreysa, *Appl. Microbiol. Biotechnol.*, 1989, **31**, 211. (*h*) G. Kreysa, D. Sell and P. Kraemer, *Ber. Bunsenges. Phys. Chem.*, 1990, **94**, 1042.

3 W. Habermann and E.-H. Pommer, *Appl. Microbiol. Biotechnol.*, 1991, **35**, 128.

4 I. Karube, T. Matsunaga, S. Tsuru and S. Suzuki, *Biotechnol. Bioeng.*, 1977, **19**, 1727.

5 (*a*) L. G. Lee and G. M. Whitesides, *J. Am. Chem. Soc.*, 1985, **107**, 6999. (*b*) I. Willner and D. Mandler, *Enzyme Microbiol. Technol.*, 1989, **11**, 467.

6 (*a*) G. Davis, H. A. O. Hill, W. J. Aston, I. J. Higgins and A. P. F. Turner, *Enzyme Microbiol. Technol.*, 1983, **5**, 383. (*b*) P. L. Yue and K. Lowther, *Chem. Eng. J.*, 1986, **33B**, 69. (*c*) S. D. Roller, H. P. Bennetto, G. M. Delaney, J. R. Mason, S. L. Stirling and C. F. Thurston, *J. Chem. Technol. Biotechnol.*, 1984, **34B**, 3.

7 B. Persson, L. Gorton, G. Johansson and A. Torstensson, *Enzyme Microbiol. Technol.*, 1985, **7**, 549.

8 (*a*) I. Willner, E. Katz, A. Riklin and R. Kasher, *J. Am. Chem. Soc.*, 1992, **114**, 10 965. (*b*) E. Katz, A. Riklin and I. Willner, *J. Electroanal. Chem.*, 1993, **354**, 129. (*c*) I. Willner, N. Lapidot, A. Riklin, R. Kasher, E. Zahavy and E. Katz, *J. Am. Chem. Soc.*, 1994, **116**, 1428. (*d*) I. Willner, A. Riklin, B. Shoham, D. Rivenzon and E. Katz, *Adv. Mater.*, 1993, **5**, 912. (*e*) B. Shoham, Y. Migron, A. Riklin, I. Willner and B. Tartakovsky, *Biosens. Bioelectron.*, 1995, **10**, 341.

9 A. N. J. Moore, E. Katz and I. Willner, *J. Electroanal. Chem.*, 1996, **417**, 189.

10 (*a*) I. Willner, E. Katz and B. Willner, *Electroanalysis*, 1997, **9**, 965. (*b*) E. Katz, V. Heleg-Shabtai, B. Willner, I. Willner and A. F. Bückmann, *Bioelectrochem. Bioenerg.*, 1997, **42**, 95.

11 (*a*) I. Willner, V. Heleg-Shabtai, R. Blonder, E. Katz, G. Tao, A. F. Bückmann and A. Heller, *J. Am. Chem. Soc.*, 1996, **118**, 10 321. (*b*) E. Katz, A. Riklin, V. Heleg-Shabtai, I. Willner and A. F. Bückmann, *Anal. Chim. Acta*, in press.

12 I. Willner, G. Arad and E. Katz, *Bioelectrochem. Bioenerg.*, 1998, **44**, 209.

13 I. Willner, E. Katz, F. Patolsky and A. F. Bückmann, *J. Chem. Soc., Perkin Trans. 2*, 1998, 1817.

14 (*a*) A. M. Klibanov, *CHEMTECH*, 1986, **16**, 354. (*b*) A. M. Klibanov, *Trends Biochem. Sci.*, 1989, **14**, 141. (*c*) J. Wang, *Talanta*, 1993, **40**, 1095.

15 T. Ruzgas, E. Csöregi, J. Emnéus, L. Gorton and G. Marko-Varga, *Anal. Chim. Acta*, 1996, **330**, 123.

16 J. Li, S. N. Tan and J. T. Oh, *J. Electroanal. Chem.*, 1998, **448**, 69.

17 L. Yang and R. W. Murray, *Anal. Chem.*, 1994, **66**, 2710.

18 (*a*) Z. Saméc, V. Marecek and J. Weber, *J. Electroanal. Chem.*, 1977, **96**, 245. (*b*) Z. Saméc, *J. Electroanal. Chem.*, 1979, **103**, 1. (*c*) Z. Saméc, V. Marecek and J. Weber, *J. Electroanal. Chem.*, 1979, **103**, 11. (*d*) J. Hanzlik, Z. Saméc and J. Hovorka, *J. Electroanal. Chem.*, 1987, **216**, 303. (*e*) G. Geblewicz and D. J. Schiffrin, *J. Electroanal. Chem.*, 1988, **244**, 27. (*f*) Y. Cheng and D. J. Schiffrin, *J. Electroanal. Chem.*, 1991, **314**, 153. (*g*) S. Kihara, *J. Electroanal. Chem.*, 1989, **271**, 107. (*h*) Y. Cheng and D. J. Schiffrin, *J. Chem. Soc., Faraday Trans.*, 1993, **89**, 199. (*i*) Y. Cheng and D. J. Schiffrin, *J. Electroanal. Chem.*, 1996, **409**, 9. (*j*) Y. Selzer and D. Mandler, *J. Electroanal. Chem.*, 1996, **409**, 15. (*k*) Z. Ding, R. G. Wellington, P.-F. Brevet and H. Girault, *J. Electroanal. Chem.*, 1997, **420**, 35. (*l*) F. Reymond, P.-F. Brevet, P.-A. Carrupt and H. Girault, *J. Electroanal. Chem.*, 1997, **424**, 121. (*m*) Y. Cheng and D. J. Schiffrin, *J. Electroanal. Chem.*, 1997, **429**, 37. (*n*) H. Ohde, K. Maeda, O. Shirai, Y. Yoshida and S. Kihara, *J. Electroanal. Chem.*, 1997, **438**, 139. (*o*) A. G. Volkov and D. W. Deamer, *Liquid–Liquid Interface. Theory and Methods*, CRC, Boca Raton, 1996.

19 (*a*) P. Vanysek and R. P. Buck, *J. Electroanal. Chem.*, 1984, **163**, 1. (*b*) J. Koryta, *Electrochim. Acta*, 1988, **33**, 189.

20 V. J. Cunnane, D. J. Schiffrin, C. Beltran, G. Geblewicz and T. Solomon, *J. Electroanal. Chem.*, 1988, **247**, 203.

21 J. Koryta and M. Skalicky, *J. Electroanal. Chem.*, 1987, **229**, 265.

22 D. J. Schiffrin, Y. Cheng, A. F. Silva, P. A. Vigato, S. Tamburini, D. Gilroy, I. Bustero and J. C. Mugica, *Hydrometallurgy*, 1994, 655.

23 H. J. Hecht, H. M. Kalisz, J. Hendle, R. D. Schmid and D. Schomburg, *J. Mol. Biol.*, 1993, **229**, 153.

24 C. Bourdillon, C. Demaile, J. Gueris, J. Moiroux and J. M. Savéant, *J. Am. Chem. Soc.*, 1993, **115**, 12264.

25 (*a*) A. Heller, *J. Phys. Chem.*, 1992, **96**, 3579. (*b*) Y. Degani and A. Heller, *J. Phys. Chem.*, 1987, **91**, 1285. (*c*) Y. Degani and A. Heller, *J. Am. Chem. Soc.*, 1988, **110**, 2615. (*d*) W. Schuhmann, T. J. Ohara, H.-L. Schmidt and A. Heller, *J. Am. Chem. Soc.*, 1991, **113**, 1394. (*e*) A. Badia, R. Carlini, A. Fernandez, F. Battaglini, S. R. Mikkelsen and A. M. English, *J. Am. Chem. Soc.*, 1993, **115**, 7053. (*f*) W. Schuhmann, *Biosens. Bioelectron.*, 1995, **10**, 181. (*g*) L. Gorton, H. I. Karan, P. D. Hale, T. Inagaki, Y. Okamoto and T. A. Skotheim, *Anal. Chim. Acta*, 1990, **228**, 23.

26 P. A. Adams, in *Peroxidases in Chemistry and Biology*, eds. J. Everse and K. E. Everse, CRC Press, Boca Raton, 1991, vol. 2, ch. 7, pp. 171–200.

27 V. Razumas, J. Kazlauskaite, T. Ruzgas and J. Kulys, *Bioelectrochem. Bioenerg.*, 1992, **28**, 159.

28 T. Lötzbeyer, W. Schuhmann, E. Katz, J. Falter and H.-L. Schmidt, *J. Electroanal. Chem.*, 1994, **377**, 291.

29 E. Katz and I. Willner, *Langmuir*, 1997, **13**, 3364.

30 O'M. Bockris and S. Srinivasan, *Fuel Cells: Their Electrochemistry*, McGraw-Hill, New York, 1969, ch. 4.

31 K. J. Vetter, *Electrochemical Kinetics*, Academic Press, New York, 1967.

32 P. Delahay, *Double Layer and Electrode Kinetics*, Interscience, Wiley, New York, 1965.

33 D. L. Morris and R. T. Buckler, in *Methods in Enzymology*, eds. J. J. Langone and H. Vunakis, Academic Press, New York, 1983, vol. 92, part E, pp. 413–417.

34 A. F. Bückmann, H. Erdmann, M. Pietzsch, J. M. Hall and J. V. Banniser, in *Flavins and Flavoproteins*, ed. K. Kuneoyagi, Walter de Gruyter, Berlin, 1994, pp. 597–609.

35 E. Katz and A. A. Solov'ev, *J. Electroanal. Chem.*, 1990, **291**, 171.

36 E. Katz, D. D. Schlereth and H.-L. Schmidt, *J. Electroanal. Chem.*, 1994, **367**, 59.

37 R. Woods, in *Electroanalytical Chemistry*, ed. A. J. Bard, Marcel Dekker, New York, 1978, vol. 9, pp. 1–162.

Paper 8/08561G